Marine Mammal Science

MARINE MAMMAL SCIENCE, 30(2): 413–432 (April 2014)

DOI: 10.1111/mms.12040

Hydrodynamic performance of the flippers of large-bodied cetaceans in relation to locomotor ecology

Paul W. Weber and **Laurens E. Howle**, Mechanical Engineering and Materials Science Department, Duke University, Durham, North Carolina 27708, U.S.A.; **Mark M. Murray**, Mechanical Engineering Department, United States Naval Academy, Annapolis, Maryland 21402, U.S.A.; **Joy S. Reidenberg**, Center for Anatomy and Functional Morphology, Icahn School of Medicine at Mount Sinai, New York, New York 10029, U.S.A.; **Frank E. Fish**,[1] Department of Biology, West Chester University, West Chester, Pennsylvania 19383, U.S.A.

Abstract

Cetaceans evolved flippers that are unique in both size and shape probably due to selection pressures associated with foraging and body size. Flippers function as control surfaces for maneuverability and stability. Flippers of cetaceans and engineered hydrofoils are similar with streamlined cross-sections and wing-like planforms, which affect lift, drag and hydrodynamic efficiency. Scale models of the flippers from large-bodied (body length >6 m) cetaceans (fin whale, killer whale, sperm whale) were constructed from computed tomography (CT) scans of flippers. Flipper planforms were highly tapered for the fin whale, a rounded, paddle-like design for the killer whale, and a square geometry for the sperm whale. Hydrodynamic properties of the models at varying angles of attack (-40° to 40°) were determined in a water tunnel with a multi-axis load cell. The flippers were found to have hydrodynamic characteristics similar to engineered wings. Differences in flipper morphology of large-bodied cetaceans and their hydrodynamic performance are associated with the requirements of aquatic locomotion involved with ecology of the whales. The flippers of the killer whale provided the greatest maneuverability, whereas the flippers of the fin whale had low drag for lunging and the flippers of the sperm whale provided lift for diving.

Key words: hydrodynamics, drag, lift, flipper, computed tomography, mysticete, odontocete, swim speed, Reynolds Number.

Cetaceans are characterized by a number of common features that are associated with hydrodynamic performance for swimming. These features include a streamlined, elongate body, propulsion by oscillation of wing-like caudal flukes, lack of external hindlimbs, and forelimbs that have been modified into flippers (Fish 1998*b*, 2004; Thewissen 1998; Reeves *et al.* 2002; Woodward *et al.* 2006; Sanchez and Berta 2010). The flippers function hydrodynamically as control surfaces that manipulate flow to generate forces for maneuverability, stability and maintenance of trim (Fish

[1]Corresponding author (email: ffish@wcupa.edu).

Report Documentation Page

Form Approved
OMB No. 0704-0188

1. REPORT DATE	2. REPORT TYPE	3. DATES COVERED
APR 2014		**00-00-2014 to 00-00-2014**

4. TITLE AND SUBTITLE	5a. CONTRACT NUMBER
Hydrodynamic performance of the flippers of large-bodied cetaceans in relation to locomotor ecology	5b. GRANT NUMBER
	5c. PROGRAM ELEMENT NUMBER
6. AUTHOR(S)	5d. PROJECT NUMBER
	5e. TASK NUMBER
	5f. WORK UNIT NUMBER
7. PERFORMING ORGANIZATION NAME(S) AND ADDRESS(ES) **West Chester University,Department of Biology,West Chester,PA,19383**	8. PERFORMING ORGANIZATION REPORT NUMBER
9. SPONSORING/MONITORING AGENCY NAME(S) AND ADDRESS(ES)	10. SPONSOR/MONITOR'S ACRONYM(S)
	11. SPONSOR/MONITOR'S REPORT NUMBER(S)

12. DISTRIBUTION/AVAILABILITY STATEMENT
Approved for public release; distribution unlimited

13. SUPPLEMENTARY NOTES

14. ABSTRACT

Cetaceans evolved flippers that are unique in both size and shape probably due to selection pressures associated with foraging and body size. Flippers function as control surfaces for maneuverability and stability. Flippers of cetaceans and engineered hydrofoils are similar with streamlined cross-sections and wing-like planforms which affect lift, drag and hydrodynamic efficiency. Scale models of the flippers from large-bodied (body length >6 m) cetaceans (fin whale, killer whale, sperm whale) were constructed from computed tomography (CT) scans of flippers. Flipper planforms were highly tapered for the fin whale, a rounded, paddle-like design for the killer whale, and a square geometry for the sperm whale. Hydrodynamic properties of the models at varying angles of attack (?40? to 40o) were determined in a water tunnel with a multi-axis load cell. The flippers were found to have hydrodynamic characteristics similar to engineered wings. Differences in flipper morphology of large-bodied cetaceans and their hydrodynamic performance are associated with the requirements of aquatic locomotion involved with ecology of the whales. The flippers of the killer whale provided the greatest maneuverability, whereas the flippers of the fin whale had low drag for lunging and the flippers of the sperm whale provided lift for diving.

15. SUBJECT TERMS

16. SECURITY CLASSIFICATION OF:			17. LIMITATION OF ABSTRACT	18. NUMBER OF PAGES	19a. NAME OF RESPONSIBLE PERSON
a. REPORT **unclassified**	b. ABSTRACT **unclassified**	c. THIS PAGE **unclassified**	**Same as Report (SAR)**	**20**	

and Battle 1995; Fish 2002, 2004; Miklosovic *et al.* 2004; Cooper *et al*. 2008; Fish *et al.* 2008; Weber *et al*. 2009*a*, *b*).

The mobile flippers act as wing-like structures to generate lift by altering angle of attack and sweep. The lift is produced by the flow dynamics over the flipper surface so that a pressure difference is produced. The pressure difference results in a net force (lift) that is oriented perpendicular to the flow direction. The flippers differ in form (*i.e.*, planform shape and size) among species in association with the ecology of each species (Fish and Battle 1995, Woodward *et al.* 2006). The planform is the projected area or shape layout of a wing-like surface. The flippers of some whales are small in relation to the rest of the body, such as those of the sperm whale and members of the beaked whales (family Ziphiidae), whereas the flippers of other whales may be as much as a third of the body's length (*e.g.*, humpback whale, *Megaptera novaeangliae*) and have a large surface area relative to the body (*e.g.*, male killer whale, *Orcinus orca*) (Fish 2004). Planforms of flippers vary from the triangular planform of the bottlenose dolphin (*Tursiops truncatus*), the rounded paddle-like planform of the killer whale, the square planform of the beluga (*Delphinapterus leucas*), the long-spanned planform with leading edge tubercles of the humpback whale, and the highly swept-back planform of the long-finned pilot whale (*Globicephala melas*). In all cases, the cross-sectional geometry of each cetacean flipper is remarkably similar to that of a modern engineered hydrofoil (Fish and Battle 1995, Weber *et al*. 2009*a*).

Foraging is one function that can place evolutionary pressure on the morphology of cetacean flippers. Mysticete whales of the family Balaenopteridae feed by engulfing large volumes of water and prey, then expelling water out through the baleen, trapping prey in the inner surface of the baleen plates (Pivorunas 1979; Goldbogen *et al.* 2006, 2007). The flippers of the minke whale (*Balaenoptera acutorostrata*) were shown to play an important role in trimming the body during feeding maneuvers (Cooper *et al*. 2008). The flippers may also play a part in facilitating in rolling maneuvers to re-orient the body and increase feeding efficiency (Goldbogen *et al*. 2006, 2012; Stimpert *et al*. 2007; Wiley *et al*. 2011). Mysticetes are able to move their flippers over a wide range and even press them against their bodies. In contrast to mysticetes, however, odontocetes have more restricted mobility of their flippers (Howell 1930, Fish 2004). The flippers of odontocetes also play an important role during feeding by aiding in turning and stabilizing the animal during high-speed hunting maneuvers while chasing prey (Fish 2002, Fish *et al*. 2003, Maresh *et al.* 2004). In addition, odontocetes that live and forage in restricted environments such as pack ice, flooded forests and rivers have flipper shapes that allow for agile maneuvers in these environments (Fish and Rohr 1999, Fish 2002).

As wing-like structures, the shape of flippers can be analyzed as engineered air- and hydro-foils to determine their effectiveness in lift generation as well as their drag performance. Flipper planforms generally have a swept-back tapered design, which varies between different species with respect to hydrodynamically relevant parameters. Advanced hydrodynamic techniques are currently used to address biological questions regarding the locomotor performance of animals (Fish and Lauder 2006). Techniques appropriate for analysis of flippers include force measurements in wind/water tunnel testing, computational fluid dynamic modeling, and flow visualization.

Previous work was performed on the hydrodynamic characteristics of cetacean flippers. Miklosovic *et al.* (2004) created an idealized model of a humpback whale flipper and determined the lift, drag, and stall characteristics *via* wind tunnel testing. They found that the elongate flippers with leading-edge tubercles of humpback whales

delay stall and enhance turning performance. Cooper *et al.* (2008) cast a minke whale flipper and tested its performance in a wind tunnel. They found that the minke whale flipper generates sufficient torque to balance the torque created from the open mouth and stabilize the body during engulfment feeding. Weber *et al.* (2009*b*) studied the hydrodynamic performance of seven different odontocete species *via* water tunnel testing, and found that swim speed was related to flipper performance. Additionally, some cetacean flippers with planforms similar to modern swept wings exhibited nonlinear lift curves in the nonstall region, which was caused by a transition from potential to vortex-dominated lift. In a separate study, Weber *et al.* (2009*a*) examined the effect of idealization (*i.e.*, constructing flipper models by using mathematical functions to describe the planform, which results in a smooth shape, and by using engineered cross-sections, which streamlines the flippers) upon cetacean flippers, and found that idealized flippers in general capture the hydrodynamic performance of real flippers.

The purpose of this study was to test the steady (*i.e.*, no flipper motion or manipulation and constant flow speed) hydrodynamic performance of the flippers of large-bodied (*i.e.*, adult body length of at least 6 m) cetaceans of the families Balaenopteridae, Physeteridae, and Delphinidae *via* water tunnel testing. As the flippers must produce forces large enough to affect the inertial mass of large-bodied whales, differences in the three-dimensional geometry of the flippers can determine their relative effectiveness for stability and maneuverability. In addition, each family has different foraging strategies and swimming behaviors that can be compared with respect to the hydrodynamics of the flipper morphologies. Hydrodynamic tests were conducted with scale models of the actual flippers of whales. It was expected that the flippers would exhibit differences in hydrodynamic performance, and that these differences would correlate with both the range of flipper shapes and the variety of foraging methods.

Materials and Methods

Flipper Collection

The flippers were removed post mortem from beach-stranded, adult whales from three species: fin whale (*Balaenoptera physalus* Linnaeus; Balaenopteridae; MMSC-01-016), killer whale (*Orcinus orca* Linnaeus; Delphinidae; HSU VM-2633) and sperm whale (*Physeter macrocephalus* Linnaeus; Physeteridae; WJW003). The flipper of the killer whale was from a female specimen. After removal, the flippers were transported to Mount Sinai School of Medicine, New York, New York (fin whale), to St. Joseph Hospital, Eureka, California (killer whale), or to Mad River Community Hospital, Arcata, California (sperm whale) and stored frozen (between –10°C and –19°C). The length of each whale was measured (BL, Table 1) during flipper removal (Table 2). Scaled digital images of the flippers were recorded to examine planform shape. Flipper planform area was determined using ImageJ software (NIH, version 1.38). The masses of the whales (m) in kg were determined from body length (BL) based on fig. 6.3 in Geraci and Lounsbury (2005).

Three-Dimensional Models

Three-dimensional models of the flippers were created by using computed tomography (CT) scans. CT scans were obtained with a Siemens Somaton Sensation at the

Table 1. List of abbreviations.

Symbol	Definition (units)
A	Planform area (m^2)
α	Angle of attack (degrees)
BL	Body length (m)
$\bar{C}$	Mean aerodynamic chord (m)
$C_{L,D}$	Lift/Drag coefficient, $C_{L,D} = \frac{F_{L,D}}{\frac{1}{2}\rho U^2 A}$ (dimensionless)
F_c	Centripetal force (N)
$F_{L,D}$	Lift/Drag force (N)
m	Mass (kg)
m_v	Virtual mass (kg)
ρ	Fluid density (kg/m^3)
ρ_s	Sea water density (kg/m^3)
r	Turning radius (m)
Re	Reynolds number, $\mathrm{Re} = \frac{U\bar{C}}{\nu}$ (dimensionless)
U	Freestream flow velocity (m/s)
ν	Kinematic viscosity (m^2/s)

Table 2. Morphometrics of cetaceans and flippers.

	Fin whale *Balaenoptera physalus*	Killer whale *Orcinus orca*	Sperm whale *Physeter macrocephalus*
Body length (m)	14.4	6.5	12.0
Mass (kg)	30,000	3,105	22,777
Virtual mass (kg)	36,000	3,726	27,332
Flipper planar area (m^2)	0.1195	0.2057	0.2739
Flipper wetted area (m^2)	0.239	0.4113	0.5477
Flipper chord (m)	0.386	0.515	0.533
Aspect ratio	3.2	1.9	1.9

Mount Sinai Medical Center, a Toshiba Aquilion 64 at St. Joseph, and a Toshiba Aquilion 16 at Mad River Community Hospital. Some thawing of the flippers occurred prior to scanning. The details for CT scanning have been provided in papers by Marino *et al.* (2003) and Fish *et al*. (2007). CT data were acquired at 100 μm slice intervals for the entire span of the flipper (*i.e.*, distance from anterior insertion of flipper with body to the distal tip). All images were provided as 512 × 512 matrix DICOM output (Digital Imaging and Communications in Medicine format).

The CT output was rendered into a file that could be read by a computer-aided design package (SolidWorks 2007, Dassault Systèmes SolidWorks Corp., Concord, MA) by using a custom-written program in C#.NET (Microsoft Corporation, Redmond, WA). Due to the limitations of the water tunnel, the models of the large cetacean flippers had to be scaled to no more than 20.3 cm in span (defined previously) and 25.4 cm in total projected length in the chordwise direction (*i.e.*, distance in the chordwise direction between the forward-most point on the flipper and rearmost point on the flipper, which is not necessarily equal to the maximum chord) to fit in the water tunnel and to minimize wall effects and tunnel blockage. The flipper models were constructed in nylon with a three-dimensional rapid prototype machine (3D Systems SinterStation HiQ Series SLS System, 3D Systems, Rock Hill, SC). Flippers were modeled from the distal tip to the midshaft of the humerus, which

approximates where the flipper would project from the body wall. The current study was limited to rigid flippers in steady flow and flipper motion was not considered. The planform shapes of all three models tested are found in Figure 1.

Flow Tank Testing

Experiments were conducted in the closed-circuit water tunnel facility at the United States Naval Academy (USNA, Annapolis, MD) Hydromechanics Laboratory in March and June of 2008. This recirculating tunnel consists of a 1.8 m long, 0.4 m × 0.4 m square test section that has a speed range of over 6 m/s. The tunnel has flow management devices that include a honeycomb flow straightener in the settling chamber and turning vanes in the tunnel corners. The freestream turbulence intensity in the test section is approximately 0.5%. Further details of the water tunnel may be found in Schultz and Flack (2005).

The flipper models (Fig. 1) were held in position inside the water tunnel with a custom-designed adjustable mounting apparatus. This apparatus held the models in a known orientation with a fixed sweep angle (*i.e.*, the tip of the flipper is pointed rearward), and allowed for changes in the angle of attack (α, incident angle of water flow to chord of model) from -90° to 90° (although testing did not require exceeding 40° in either direction). The blockage (*i.e.*, ratio of presented area in flow direction to test section area) was 2% for all models at α of 0° in the water tunnel with a cross-sectional area of 0.16 m. At the highest α (-40°, 40°), the maximum blockage was 11% for the sperm whale flipper model.

The forces (lift and drag) on the flipper models were measured either with a load cell or with block gauges depending upon the testing speed. The load cell was an Advanced Mechanical Technology, Inc. Dynamometer Model UDW3-6-1000 (AMTI, Watertown, MA), specifically designed for underwater use. The block gauges were Modular-Force (Block) Gage Models HI-M-2 (Hydronautics, Inc., Fulton, MD). The load cell provided more accurate force readings, but was limited to relatively low testing speeds (model dependant but generally <4 m/s); conversely, the block gauges allowed for the measurement of larger flipper forces (caused by higher tunnel speeds) but at the expense of reduced accuracy. Data were acquired using LabVIEW version 8.0 (National Instruments, Austin, TX), and the data were postprocessed using a custom-written program in C#.NET. The experimental procedure consisted of allowing the water tunnel to stabilize at the test speed, positioning the flipper model to the desired α, collecting the data at that angle, then manually repositioning the model to the next α.

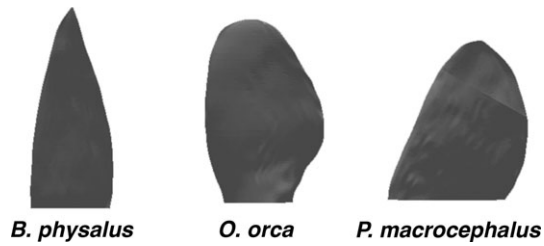

Figure 1. Planform shapes of fin whale (*Balaenoptera physalus*), killer whale (*Orcinus orca*), and sperm whale (*Physeter macrocephalus*). Flippers are oriented with the leading edge facing left.

Data are reported in terms of the lift (C_L) and drag (C_D) coefficients:

$$C_{L,D} = \frac{F_{L,D}}{\frac{1}{2}\rho U^2 A} \quad (1)$$

where $F_{L,D}$ is the measured lift/drag force (N), ρ is the (incompressible) fluid density (kg/m^3), U is the water tunnel speed (m/s) and A is the planform area of the flipper model (m^2).

Dynamic similarity was achieved between the models and actual flippers (Shaughnessy *et al.* 2005) by matching the Reynolds number (Re):

$$Re = \frac{U\bar{C}}{v} \quad (2)$$

where U is the flow speed (m/s), $\bar{C}$ is the mean aerodynamic chord (m), and v is the kinematic viscosity (m^2/s). Fluid kinematic similarity was obtained by ensuring both geometric and dynamic similarity between the model and the flipper.

Equation (2) was used to determine appropriate water tunnel testing speeds given the geometric parameters and water temperatures of both the model and animal. Two different testing speeds were calculated for each flipper model, and these speeds were chosen in a manner that allowed for a baseline comparison between species. Each water tunnel model was first tested at a speed equivalent to an animal swim speed of 2 m/s and will be hereafter referred to as "swim speed match" cases. A speed of 2 m/s was chosen because field observation and data have confirmed that all animals from which models were made were known to be able to swim at this speed. Note that since flippers are used for flow control and not propulsion, the flow speed over the flipper is equal to the animal swim speed. The models were then tested at a speed to achieve a Re of 250,000, and will be hereafter referred to as "Re match" cases. Note that matching the swim speed of 2 m/s ensures that the Re for the model and the animal are the same, although for the swim speed match this Re is not necessarily equal to 250,000 (Table 3 lists the values of Re for each animal at the 2 m/s swim speed). For the large cetacean models tested in this study, the calculated speed for the Re match was always lower than the swim speed match.

Additional factors that led to the choice of 2 m/s as the swim speed match and 250,000 as the Re match included limitations of the water tunnel and of the load cell, and consideration of low-speed fluid dynamic effects. To elaborate, if the swim

Table 3. Select hydrodynamic performance parameters for the cetacean flipper models at 2 m/s swim speed match trials.

Parameter	Fin whale *Balaenoptera physalus*	Killer whale *Orcinus orca*	Sperm whale *Physeter macrocephalus*
$C_{L,\max}$	1.452	1.040	0.897
$\alpha_{C_{L,\max}}$(deg)	31	23	19
$C_{D,\min}$	0.0545	0.0356	0.0361
$\alpha_{C_{D,\min}}$(deg)	−2	0	−1
C_L curve slope (deg^{-1})	0.0649	0.0575	0.0537
$(C_L/C_D)_{\max}$	6.18	4.63	5.65
Re at testing speed	398,000	674,000	872,000

speed or Re was chosen at a value that was too low, then the load cell would have difficultly resolving the resulting small forces, and low Re fluid dynamic effects (such as laminar boundary layer detachment and reattachment, and thick boundary layers) would have to be considered. If the swim speed or Re was chosen at a value that was too high, then the speed capabilities of the water tunnel could possibly be exceeded, and a nonrealistic value of the animal swim speed (*i.e.*, a speed that is faster than the animal is actually able to swim in the wild) may result.

The large whales considered in this study presented special challenges with regards to water tunnel testing. Size restrictions of the USNA water tunnel required that all of the flipper models be scaled down. As a consequence of this, equation (2) requires that the water tunnel testing speed be increased by a factor of (model scale)$^{-1}$. In order to obtain similarity in the water tunnel between the models and real flippers for higher values of the swim speeds in the wild, the testing speeds would far exceed the capability of the water tunnel.

Experimental error analysis was conducted using standard techniques (Fox and McDonald 1999). Sources of error in the experiment included uncertainties in the Pitot tube voltage reading and calibration curve, uncertainties in the load cell/block gauge readings, uncertainties in reading water temperature and in tabulated values of kinematic viscosity based on the water temperature, and uncertainties in geometry due to the model construction process (including both three-dimensional printer construction error and geometry changes due to painting/sanding). These individual uncertainties propagate into overall uncertainties for quantities that depend upon them, which the error analysis takes into account. The analysis determined that the maximum uncertainty in the water tunnel speed was $\pm 1.3\%$, the maximum uncertainty in the Re was $\pm 3.2\%$, and the maximum uncertainty in C_L and C_D measurements was $\pm 6.7\%$.

Full Scale Analysis

Morphological and hydrodynamic data (Table 2, 3) were used to determine turning maneuver performance (surfacing, diving, lateral turn) for full-scale whales swimming at 2 m/s. The centripetal force (F_c) generated for maneuvering was calculated from equation 1 for the maximum lift (F_L) provided by the two flippers in which:

$$F_C = F_L = [2(0.5\rho_S U^2 A)C_{L,\max}] \tag{3}$$

where ρ_s is the density of sea water (1,024 kg/m^3) and $C_{L,\max}$ is the maximum lift coefficient for either positive or negative α from Table 3. Positive values of $C_{L,\max}$ were used to estimate F_c for surfacing performance, whereas negative values of $C_{L,\max}$ were used to estimate F_c for diving performance for all three species. As only the killer whale could effectively adduct its flippers (Fish 2002, Cooper *et al.* 2008), lateral turn performance was computed only for this species. In this case, it was considered that F_c was generated from one flipper at a positive α and the other flipper at a negative α.

The radius of the turns (r) was calculated as:

$$r = m_v U^2 / F_c \tag{4}$$

where m_v is the virtual mass. m_v is equal to the mass of the whale plus 20% of the body mass. This extra mass is considered to be the additional mass of water that is

entrained to the body of the animal due to the viscosity of the fluid (Webb 1975). For comparison, turn radius was calculated for absolute values and relative values (r/L).

Results

The planforms of the flippers differed among the representatives of the three cetacean families studied (Table 2, Fig. 1). The fin whale had highly tapered flippers with a relatively high aspect ratio {(flipper span)^2/planform area} of 3.2. The flippers of the killer whale and sperm whale were rounded with aspect ratios of 1.9. CT scans of the flippers showed that the cross-sections had conventional streamlined profiles (Fig. 2). These profiles were characterized by having a rounded leading edge and a long tapering trailing edge.

The experimental hydrodynamic data were corrected for the finite tunnel effects of the presence of walls and solid blockage by the models as outlined in Barlow *et al.* (1999). The walls of the tunnel produce upwash upon the model, which changes the effective α. Solid blockage is caused by the local water tunnel cross-sectional area being decreased in the vicinity of the model, which means that the average local flow velocity must increase. For all models tested, the maximum change in C_L due to finite tunnel effects was 0.213 (17%), the maximum change in C_D was 0.194 (19%), and the maximum change in α was 2.2°.

Lift data are presented in Figure 3, and Tables 3 and 4. No clear trend was found with regards to $C_{L,\max}$, as the fin whale had the highest value and the sperm whale

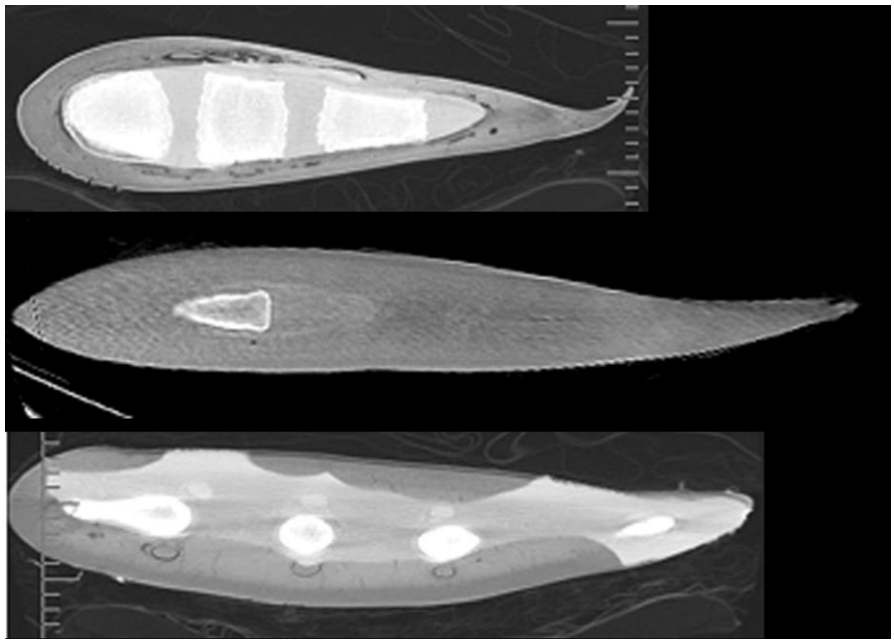

Figure 2. Cross-sectional profiles from the mid-span of cetacean flippers obtained from CT scans. The flippers are arranged from top to bottom as fin whale (*Balaenoptera physalus*), killer whale (*Orcinus orca*), and sperm whale (*Physeter macrocephalus*).

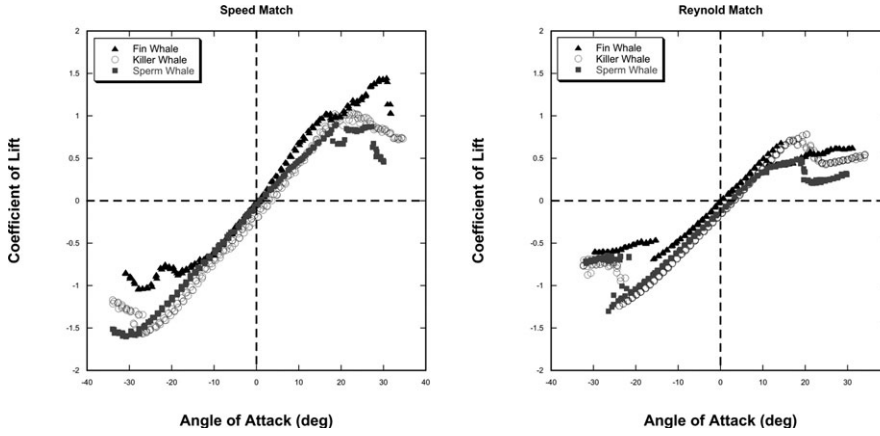

Figure 3. Lift coefficient *vs.* angle of attack for 2 m/s speed match trial (left) and Re = 250,000 match trial (right).

Table 4. Select hydrodynamic performance parameters for the cetacean flipper models tested for Re = 250,000 match trials.

Parameter	Fin whale *Balaenoptera physalus*	Killer whale *Orcinus orca*	Sperm whale *Physeter macrocephalus*
$C_{L,\max}$	0.689	0.784	0.489
$\alpha_{C_{L,\max}}$(deg)	14	20	18
$C_{D,\min}$	0.0510	0.0441	0.0522
$\alpha_{C_{D,\min}}$(deg)	−1	−1	1
C_L curve slope (deg^{-1})	0.0469	0.0505	0.0473
(C_L/C_D)max	4.57	4.00	3.71
Speed at Re = 250,000 (m/s)	1.26	0.742	0.574

had the lowest value for the swim speed match trial with positive α, while the sperm whale had the highest value for negative α and the fin whale had the lowest value. For the Re match trial, $C_{L,\max}$ was highest for the killer whale and lowest for the sperm whale with a positive α, but the sperm whale was highest and the fin whale was the lowest with a negative α.

The α at which the maximum C_L was attained for both positive and negative angles was $\alpha_{C_{L,\max}}$ and indicates the angle at which stall occurs. Stall refers to the phenomenon where there is a dramatic loss of lift with increased α. Stall occurs after the maximum value of lift coefficient ($C_{L,max}$) is obtained. $\alpha_{C_{L,\max}}$ either stayed the same or decreased for all animals from the swim speed to the Re match trials. Stall angles varied from 14.3° to 20.4° and −27.9° to −30.8° for swim speed match and 14.3° to 20.4° and −15.8° to −26.4° for Re match. With the exception of the fin whale for swim speed match, $\alpha_{C_{L,\max}}$ was higher at negative angles than at positive angles. The most drastic change was for the fin whale, where $\alpha_{C_{L,\max}}$ decreased by 17° between the swim speed and Re match trials. Re effects appear to be important for the slow swim speeds considered in this study. The range of α between positive and negative stall was >30° for all species.

The C_L curve slope was found to be linear in the region before reaching $\alpha_{C_{L,\max}}$ for all animals (Fig. 3). The fin whale had both the greatest (swim speed match) and least (Re match) C_L curve slope. All animal models saw their C_L curve slope decrease from the swim speed to the Re match trials (greatest decrease was the fin whale where the Re match value was only 72% of the swim speed match value).

Drag data are presented in Figure 4, and Tables 3 and 4. $C_{D,min}$ for killer whale was lowest for swim speed and Re match trials, $C_{D,min}$ increased between the swim speed and Re match trials for killer whale and sperm whale models, whereas the fin whale showed a 5.9% decrease. The sperm whale exhibited the greatest increase between trials, with $C_{D,\min}$ for the Re match trial being 145% of its value from the swim speed match trial. For all animals, the average $C_{D,\min}$ occurred in the α range of $-2 \leq \alpha \leq 1$, with slight (no more than 2° if at all) variation between trials.

Efficiency is defined as C_L/C_D (or alternatively Lift/Drag), and it is one method to quantitatively judge the performance of a lifting surface (Anderson 2001). Data for hydrodynamic efficiency are presented in Figure 5, and Table 3 and 4. Killer whale was found to have the highest maximum value of efficiency $(C_L/C_D)_{\max}$ for both trials, followed by sperm whale. The positive α at which $(C_L/C_D)_{\max}$ occurred was between 9.5° (killer whale) and 11.7° (sperm whale) for the swim speed match trial, and was between 10.9° (sperm whale) and 11.9° (killer whale) for the Re match trial; whereas the negative α at which $(C_L/C_D)_{\max}$ occurred was between −5.0° (killer whale) and −7.9° (fin whale) for the swim speed match trial, and was between −9.3° (killer whale) and −9.5° (sperm whale) for the Re match trial. The sperm whale had the largest drop in efficiency between the two trials, with its Re match value only being 66% of its speed match value.

Full scale analysis indicated that fin whale had the lowest absolute centripetal forces (F_c) produced by its flippers when surfacing (710.6 N) and diving (508.6 N), whereas sperm whale had the highest with 1,006.3 N and 1,796.8 N for surfacing and diving, respectively. Higher F_c values were computed for diving than surfacing maneuvers for killer whale and sperm whale, whereas the fin whale showed the opposite trend.

The turn radius for surfacing and diving by fin whale was over 1.8 times greater than the radii computed for sperm whale and over 11.9 times greater than for killer

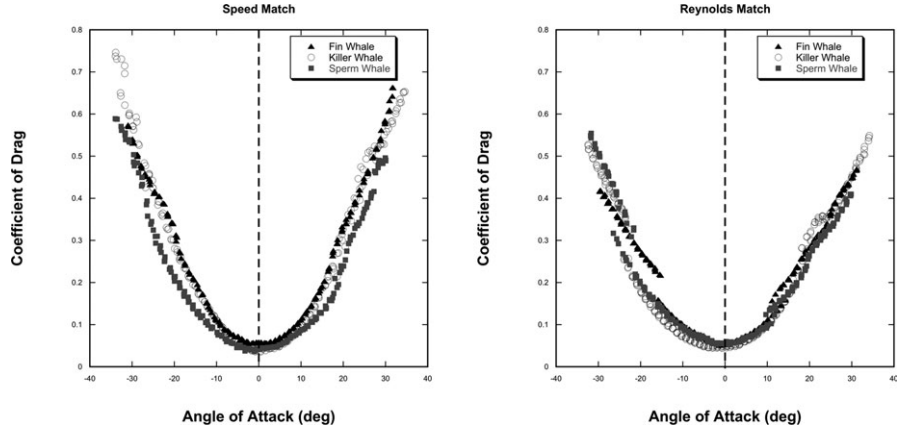

Figure 4. Drag coefficient *vs.* angle of attack for 2 m/s speed match trial (left) and Re = 250,000 match trial (right).

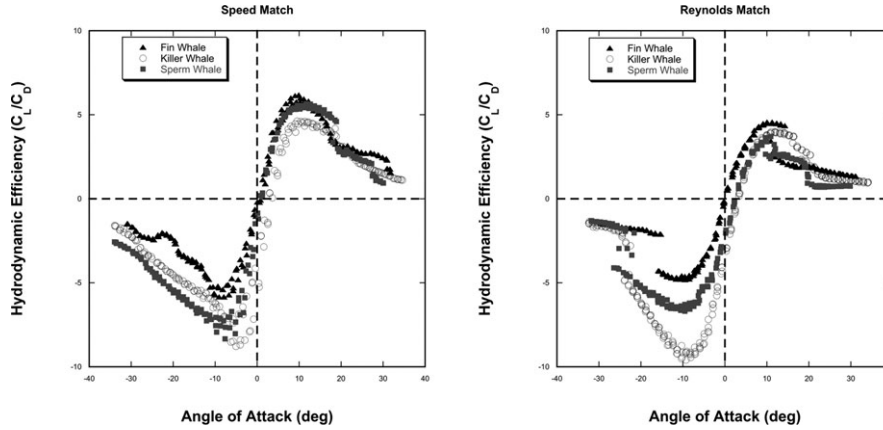

Figure 5. Efficiency *vs.* angle of attack for 2 m/s speed match trial (left) and Re = 250,000 match trial (right).

whale (Table 5). When scaled by body length (*BL*), the greatest turning radius (19.6) was shown for fin whale when diving. The smallest diving radius of 1.7 occurred for killer whale. The combined F_c for both flippers of killer whale during lateral turns was 1,102.3 N (Table 5). The computed lateral turning radius was 13.5 m and 2.1 when scaled to body length.

Discussion

Cetaceans evolved control surfaces to swim, maneuver, and stabilize the body (Fish 2002). These control surfaces include the dorsal fin, caudal peduncle, caudal flukes, and pectoral flippers (Fish 2002, Fish *et al*. 2008). The flippers of cetaceans are the most versatile of the control surfaces. The flippers comprise 14%–42% of the total control surface area (Fish and Rohr 1999) and have a ball and socket articulation that permits three degrees of freedom (*i.e.*, flexion-extension, abduction-adduction, rotation) (Felts 1966, Berta *et al*. 2006). The mobility of the flippers makes these appendages important for stability (*i.e.*, trim control, reduction of recoil from propulsive movements) and maneuverability (*i.e.*, turning, diving surfacing, braking). Biomechanically, the flippers act like a pair of wings to generate lift and control flow

Table 5. Absolute values of turn radius in meters and turn radius relative to body length computed at a swim speed of 2 m/s associated with maneuvering behavior.

	Fin whale *Balaenoptera physalus*	Killer whale *Orcinus orca*	Sperm whale *Physeter macrocephalus*
Behavior	Turn radius (*r*/*BL*)		
Surfacing	202.6 (14.1)	17.0 (2.6)	108.7 (9.1)
Diving	283.2 (19.6)	11.2 (1.7)	60.9 (5.1)
Lateral turn	–	13.5 (2.1)	–

(Edel and Winn 1978; Fish 2002, 2004; Fish and Lauder 2006). The effectiveness of such lifting surfaces is dependent on the hydrodynamic characteristics (*i.e.*, lift, drag, stall) of the design. It is considered that the diversity of cetacean pectoral flipper morphologies evolved with respect to each species' ecology (Benke 1993, Woodward *et al.* 2006).

Cetaceans are among the largest living aquatic animals on the planet. Within Mysticeti, the blue whale (*B. musculus*) can reach a maximum length of 33.6 m and is the largest cetacean (Yochem and Leatherwood 1985) with the fin whale as the second largest at 27.0 m (Gambell 1985). For Odontoceti, the sperm whale can be as large as 18.3 m (Rice 1989), and although comparatively smaller in size, killer whales are the largest of the Delphinidae. Male killer whales can reach a length of 6.75 m and weigh 5,568 kg (Dahlheim and Heyning 1999). The ecology of the three species in the current study differ in regard to flipper morphology and swimming performance for speed, diving, and maneuverability that is associated with feeding and prey selection.

Flipper shape, as indicated by its planform, is described as either paddle-like or wing-like (Sanchez and Berta 2010). Paddle-like flippers are relatively short and broad with a rounded or squared tip (*e.g.*, killer whale, sperm whale), whereas, wing-like flippers are relatively long and narrow with tapered and pointed tips (*e.g.*, fin whale). Such wing-like designs can produce high lift with low drag.

Flipper cross-sections have a streamlined, fusiform design analogous to engineered high-performance aerofoils and hydrofoils (Fig. 2) (Edel and Winn 1978, Fish and Battle 1995). Streamlining aids in minimizing drag. The streamlined profile is characterized by a rounded leading edge, slowly tapering tail, and a Thickness Ratio (*TR* = maximum thickness to maximum length) of 0.14–0.33 (Webb 1975, Blake 1983). The optimal *TR* is 0.22, which provides minimum drag (von Mises 1945). Streamlining reduces the magnitude of the pressure gradient over the flipper and delays separation of the boundary layer from the flipper. Separation occurs closer to the trailing edge resulting in a narrow wake and reduced drag. Flow visualization experiments with gliding dolphins showed a lack of separation over the flipper surface (Rohr *et al.* 1995, 1998). Delaying separation as the flipper is canted at an angle to the on-coming flow (*i.e.*, α) delays stall with its loss of lift and increased drag to higher angles.

The highly tapered, high aspect ratio flippers of the fin whale and other balaenopterids are associated with swimming at high speeds, particularly during lunge feeding (Bose and Lien 1989, Fish and Rohr, 1999, Goldbogen *et al.* 2006). The fin whale can swim at speeds over 10.3 m/s (Gambell 1985), but routinely swim and lunge feed at 1.5–4.0 m/s (Tomilin 1957, Williamson 1972, Goldbogen *et al.* 2007). The flippers of fin whale are relatively small at approximately 0.08–0.10 times the length of the body (Gambell 1985). The flippers can be abducted so that they are oriented perpendicular to the longitudinal axis of the body (*i.e.*, sweep angle of zero), like certain airplane wings. The flipper can also be fully adducted so that the trailing edge touches the body (*i.e.*, increased sweep angle, see below), or adducted with medial rotation so that its flat ventral surface is pressed against the body. This latter orientation occurs during normal swimming to reduce drag. Flipper rotation in the abducted position allows adjustments to lift while swimming. Flipper abduction is used to help maintain trim during engulfment feeding to counter the downward pitching moment due to the increased drag from depression of the lower jaw and expansion of the ventral pouch (Pivorunas 1979; Goldbogen *et al.* 2006, 2007; Cooper *et al.* 2008). These whales feed by engulfing whole shoals of small fish and euphausiids, requiring minimal maneuvering (Woodward *et al.* 2006). The flippers may be involved in a rolling maneuver as occurs in other balaenopterids. The blue

whale is capable of 360° rolls, which are used to position the whale with respect to krill patches to maximize prey capture (Goldbogen *et al*. 2012).

Similar to the mobility of balaenopterid flippers, flippers of the sperm whale have a range of motion that includes abduction, adduction, and rotation (Whitehead 2003). It is unknown how the flippers are used during foraging. However, the flippers of this species may be of limited use due to their relatively small size and the sperm whale's diving behavior. Dives to depths of over 1,000 m can be nearly vertical, requiring almost no maneuvering (Whitehead 2003, 2009). Routine swimming speeds by sperm whales are slow at 0.7–2.8 m/s (Tomilin 1957, Papastavrou *et al*. 1989, Watkins *et al*. 1993).

The sperm whale feeds primarily on squid by suction feeding (Berta *et al.* 2006). The rounded, low aspect ratio planform indicates use during low speed maneuvering (Woodward *et al.* 2006). Use of the flippers may be involved with rolling maneuvers (Miller *et al*. 2004). Like the balaenopterids, rolling could be involved with repositioning the jaws during interactions with prey (Goldbogen *et al*. 2012). However, the relative inflexibility of the body and ankylosed cervical vertebrae would limit maneuverability for active pursuit of prey (Norris and Møhl 1983, Rice 1989).

The flipper shape of the killer whale may be an adaptable, generalized morphology associated with its differing hunting techniques, varied prey, and the diverse habitats. These animals prey on schooling fish and marine mammals, including the sperm whale and large mysticetes (Evans 1987, Estes *et al*. 1998, Pitman *et al.* 2001, Springer *et al*. 2003). Killer whales hunt singly or in packs, use high-speed chases, rapid maneuvers, concealment, encircling the prey, ramming, body slams, intentional stranding, and percussive displays (*i.e*., slapping the water with the flippers and flukes) (Similä and Ugarte 1993, Flórez-González *et al*. 1994, Guinet and Bouvier 1995, Barrett-Lennard *et al*. 1996, Similä 1997, Pitman *et al*. 2003, Ford 2009, Pitman and Durban 2012). Killer whales forage in open water or along complex environments of shorelines and pack ice.

Killer whales are capable of swimming speeds over 7 m/s (Johannessen and Harder 1960, Fish 1998*a*, Fish and Rohr 1999) and can perform high-speed maneuvers, despite possessing broad flippers with a low aspect ratio, which are typically indicative of a slow maneuvering species (Woodward *et al*. 2006). Killer whales can turn at a maximum rate of 233°/s at 6 m/s within a radius of 0.11 body lengths by using the flippers in combination with peduncle, and flukes (Fish 2002). Mature male killer whales have disproportionately large flippers that are 1.7 times longer than females (Clark and Odell 1999, Ford 2009). This size differential can be associated with sexual differences in hunting and maneuvering performance by transient killer whales, as the females are mainly responsible for corralling prey (Pitman *et al*. 2001, Barrett-Lennard and Heise 2006). Often females and subadults execute turning lunges on large prey species, while adult males often remain at a distance until the prey is disabled (Jefferson *et al*. 1991, Barrett-Lennard and Heise 2006). The relatively large size of the male flippers and body may be a detriment to maneuverability and reflect a sexually selected characteristic.

The C_L and C_D *vs.* α curves for all the species examined were similar to those of typical modern engineered hydrofoils or airfoils (von Mises 1945, Abbott and von Doenhoff 1959, Anderson 2001). However, as the flippers were modeled after real flippers, the curves obtained were not as smooth as the curves for an engineered foil. C_L curves for all flippers had linear C_L curve slopes below the stall angle $(\alpha_{C_{L,\max}})$ (Fig. 3, see below). C_D curves were bucket shaped (parabolic), with a defined $\alpha_{C_{D,\min}}$ (Fig. 4). Drag values for the flipper models (0.0361–0.0545) were higher than values

for engineered foils with similar profiles (NACA 654-021; $C_{D,\min} = 0.004$; Abbott and von Doenhoff 1959). Engineered foils have highly streamlined cross-sections that are purposefully designed to minimize drag.

All flipper models exhibited stall characteristics typical of engineered hydrofoils (von Mises 1945, Abbott and von Doenhoff 1959). Physically, stall is due to large regions of reversed flow and flow separation along the flipper surface as α is increased. This flow causes a decrease in the pressure differential between the two sides of the wing, thereby decreasing lift. A further increase in α results in a decrease in the lifting force (Anderson 2001). The $\alpha_{C_{L,\max}}$ was lowest for the fin whale Re match trial (14°), but highest for the swim speed match trial (31°). Overall, the sperm whale had values of $\alpha_{C_{L,\max}}$ that were consistently lower than the other two whales. Furthermore, the loss of lift for the fin whale was abrupt at stall for positive α, while the killer whale flipper stalls very gradually. The phenomenon of tip stall (*i.e.*, tip of wing stalls before the main body of the wing) was also observed for some models, where part of the flipper stalls and causes a subsequent decrease in the C_L curve slope near $C_{L,\max}$, but the flow still remains largely attached and therefore the value of the C_L curve continues to increase at a lower rate until fully stalled. The sperm whale $C_{L,\max}$ curve is an example of this trend (Fig. 3).

The hydrodynamic performance of the fin whale flipper in this study differed from the performance of the minke whale flipper reported by Cooper *et al.* (2008). Most notably, the fin whale flipper stalled at $\alpha = 14°–31°$ for both trials, while Cooper *et al.* (2008) reported stall from $\alpha = 6°–12°$. $C_{L,\max}$ values reported in Cooper *et al.* (2008) were also higher (1.27–1.62) than they were for the present study (0.69–1.45). These differences are explained by the differing sweep of the flippers between the two studies.

The flipper in the Cooper *et al.* (2008) study was tested at a sweep angle of zero (*i.e.*, flipper abducted laterally so it protrudes directly perpendicular from the body), whereas the flipper of this study had a sweep angle of approximately 45° (Fig. 1). Generally, the maximum lift decreases and α at stall increases with increasing sweep angle (Hoerner and Borst 1985, Bertin and Smith 1998, Murray *et al*. 2005), which is consistent with observations here. In the wild, the minke whale displays a flipper sweep angle of zero during gulping maneuvers, while a sweep angle of 45° is observed during swimming or cruising (Cooper *et al.* 2008). Another difference between measurements on the flippers of minke and fin whales is accounted for by the different values of Re that were tested. Cooper *et al*. (2008) tested a range of Re values between 171,002 and 592,574, whereas the values of Re tested for the fin whale were 250,000 and 398,000. However, both this study and Cooper *et al.* (2008) found $C_{L,\max}$ to similarly decrease with increasing Re and the drag values measured for both studies were comparable.

The overall hydrodynamic performance was generally greater for the fin whale with high aspect ratio flippers compared to the paddle-like flippers of killer whale and sperm whale. For positive α, the hydrodynamic efficiency, $(C_L/C_D)_{\max}$, for fin whale was 14%–23% and 8%–22% higher than for killer whale and sperm whale. High aspect ratio wings produce high lift with low drag with high propulsive efficiency.

The differences between the various morphologies displayed in this study, although apparent, showed considerable overlap in hydrodynamic performance. Similarly, the hydrodynamic data displayed similarities in performance with the flippers of small cetaceans of the Iniidae, Delphinidae, Kogiidae, and Phocoenidae (Weber *et al.* 2009*b*). Both the large and small cetacean studies are directly comparable as they both used the same techniques and flow conditions. At a matched speed of 2 m/s, the large whales had a mean $C_{L,\max}$ of 1.130 (SD = 0.288), whereas the smaller

cetaceans had an average $C_{L,\max}$ of 1.140 (SD = 0.180). Comparing drag characteristics, the large whales had an average $C_{D,\min}$ of 0.042 (SD = 0.011), while the average $C_{D,\min}$ of 0.039 (SD = 0.016) for the smaller cetaceans.

Although relationships between hydrodynamic performance and flipper morphology are evident (*i.e.*, aspect ratio, planform, streamlined profile) for cetaceans, the ecological performance and hydrodynamics of the flippers are apparent only when the absolute values for lift and drag are calculated. The usefulness of the flippers for maneuvering by the fin whale is small, compared to the other two species. Such low performance is related to the feeding behavior of the fin whale, which surges straight ahead to engulf prey (Goldbogen *et al*. 2006, 2007). High-speed turning maneuvers are not part of the behavioral repertoire of the second largest whale. The flippers would be used to aid in stabilizing the trim on the body upon inflation of the throat pouch during feeding (Cooper *et al*. 2008) and in surfacing and diving in conjunction with the flukes.

Based on the hydrodynamic characteristics of the flippers, the maneuvering performance of sperm whale probably corresponds with their diving behavior. The flippers have a relatively small size, low $C_{D,\min}$ and the ability to be pressed against the body, which would reduce the drag when gliding during ascents and descents (Miller *et al*. 2004). The dive profile for sperm whale is "U-shaped" with sudden changes in depth (Lockyer 1977, Whitehead 2003, Zimmer *et al*. 2003). This performance would be facilitated by the smaller radius turns compared to fin whale. However, the ability to maneuver by sperm whale is still limited. The use of feeding techniques, including suction and the controversial sonic stunning, may compensate for the whale's inflexibility of the body and limited mobility relative to their smaller, elusive prey (*e.g.*, squid) (Norris and Harvey 1972, Norris and Møhl 1983, Werth 2004).

The killer whale was the most maneuverable of the three whales examined. The length-specific turn radius (r/BL) for killer whale was 18.4% and 8.7% surfacing and diving maneuvers by fin whale, respectively, and 28.6% and 33.3% of surfacing and diving maneuvers computed for sperm whale, respectively. Furthermore articulation and placement of the flippers of killer whale permits enhanced mobility for use in lateral turns. However, the relative turn radius was 19 times greater than observed by Fish (2002). This difference in turning performance is explained by the use of flukes and peduncle in the maneuvers (Fish 2002). The ability to perform rapid and tight lateral turns, dives, and ascents allows killer whales to surround and out-maneuver prey during attacks (Campbell *et al*. 1988, Silber *et al*. 1990, Similä 1997, Pitman *et al*. 2003).

In summary, we found that the flippers of three large cetaceans from Balaenopteridae, Physeteridae, and Delphinidae exhibited lift and drag curves that are similar both to engineered foils and results reported in earlier studies. When flipper sizes, planforms, cross-sectional profiles and hydrodynamic characteristics are considered collectively to determine the forces generated by the flippers, the projected swimming performance is shown to be associated with the ecology of each distinct species. The large cetaceans have unique hunting and feeding methods that require the generation of lift for stability and maneuverability while reducing drag.

Acknowledgments

This work was supported by the National Science Foundation through grant number IOS-0640185 to FEF (principal investigator), LEH and MMM, and the technical support staff of

the United States Naval Academy. JSR was supported by a grant from the Office of Naval Research and a NOAA Prescott Marine Mammal Stranding Grant. PWW was supported by the National Defense Science and Engineering Graduate (NDSEG) Fellowship through the Office of Naval Research. The authors would like to thank Aracelis Perez of Radiology Associates, Mount Sinai Medical Center, New York, for arranging/performing CT scanning of the fin whale flipper; Stacy Wallis at St. Joseph Hospital, Eureka, California, for arranging/performing CT scanning of the killer whale flipper, and David Wellman at Mad River Community Hospital, Arcata, California, for arranging/performing CT scanning of the sperm whale flipper. Thanks are also given to members of the National Marine Mammal Stranding Network for providing access for J.S.R. to obtain specimens from beach stranded whales; in particular, the Marine Mammal Stranding Center, Brigantine, New Jersey; Mystic Aquarium, Mystic, Connecticut; Riverhead Aquarium and Research Foundation, Riverhead, New York; Virginia Aquarium and Marine Science Center, Virginia Beach, Virginia. We appreciate the invaluable assistance of Jeff Jacobsen of the Vertebrate Museum of Humboldt State University, California, the United States Coast Guard, and the United States Army Corps of Engineers (specifically the Caven Point Facility, Port Liberty, New Jersey) in locating and recovering ship-struck specimens and facilitating their dissections. We also wish to thank Janet Fontanella and the three anonymous reviewers for their assistance with the manuscript.

Literature Cited

Abbott, I. H., and A. E. von Doenhoff. 1959. Theory of wing sections. Dover, New York, NY.

Anderson, J. D. 2001. Fundamentals of aerodynamics. McGraw-Hill, Boston, MA.

Barlow, J. B., W. H. Rae and A. Pope. 1999. Low-speed wind tunnel testing. 3rd edition. John Wiley & Sons, Inc., New York, NY.

Barrett-Lennard, L. G., J. K. B. Ford and K. A. Heise. 1996. The mixed blessing of echolocation: Differences in sonar use by fish-eating and mammal-eating killer whales. Animal Behaviour 51:553–565.

Barrett-Lennard, L. G., and K. A. Heise. 2006. The natural history and ecology of killer whales. Pages 163–173 *in* J. A. Estes, D. P. Demaster, D. F. Doak, T. M. Williams and R. L. Brownell, Jr, eds. Whales, whaling, and ocean ecosystems. University of California Press, Berkeley, CA.

Benke, H. 1993. Investigations on the osteology and the functional morphology of the flipper of whales and dolphins (Cetacea). Investigations on Cetacea 24:9–252.

Berta, A., J. L. Sumich and K. M. Kovacs. 2006. Marine mammals: Evolutionary biology. Academic Press, Amsterdam, The Netherlands.

Bertin, J. J., and M. L. Smith. 1998. Aerodynamics for engineers. Prentice Hall, Upper Saddle River, NJ.

Blake, R. W. 1983. Fish locomotion. Cambridge University Press, Cambridge, U.K.

Bose, N., and J. Lien. 1989. Propulsion of a fin whale (*Balaenoptera physalus*): Why the fin whale is a fast swimmer. Proceedings of the Royal Society of London B 237:175–200.

Campbell, P. R., D. B. Yurick and N. B. Snow. 1988. Predation on narwhals, *Monodon monoceros*, by killer whales, *Orcinus orca*, in the Eastern Canadian Arctic. Canadian Field-Naturalist 102:689–696.

Clark, S. T., and D. K. Odell. 1999. Allometric relationships and sexual dimorphism in captive killer whales (*Orcinus orca*). Journal of Mammalogy 80:777–785.

Cooper, L. N., N. Sedano, S. Johannson, *et al.* 2008. Hydrodynamic performance of the minke whale (*Balaenoptera acutorostrata*) flipper. Journal of Experimental Biology 211:1859–1867.

Dahlheim, M. E., and J. E. Heyning. 1999. Killer whale *Orcinus orca* (Linnaeus, 1758). Pages 281–322 *in* S. H. Ridgway, and R. Harrison, eds. Handbook of marine mammals. Academic Press, San Diego, CA.

Edel, R. K., and H. E. Winn. 1978. Observations on underwater locomotion and flipper movement of the humpback whale *Megaptera novaeangliae*. Marine Biology 48: 279–287.

Estes, J. A., M. T. Tinker, T. M. Williams and D. F. Doak. 1998. Killer whale predation on sea otters linking coastal with oceanic ecosystems. Science 282:473–476.

Evans, P. 1987. The natural history of whales and dolphins. Christopher Helm Publishing, London, U.K.

Felts, W. J. L. 1966. Some functional and structural characteristics of cetacean flippers and flukes. Pages 255–276 *in* K. S. Norris, ed. Whales, dolphins, and porpoises. University of California Press, Berkeley, CA.

Fish, F. E. 1998*a*. Comparative kinematics and hydrodynamics of odontocete cetaceans: Morphological and ecological correlates with swimming performance. Journal of Experimental Biology 201:2867–2877.

Fish, F. E. 1998*b*. Biomechanical perspective on the origin of cetacean flukes. Pages 303–324 *in* J. G. M. Thewissen, ed. The emergence of whales: Evolutionary patterns in the origin of Cetacea. Plenum Press, New York, NY.

Fish, F. E. 2002. Balancing requirements for stability and maneuverability in cetaceans. Integrative and Comparative Biology 42:85–93.

Fish, F. E. 2004. Structure and mechanics of nonpiscine control surfaces. IEEE Journal of Oceanic Engineering 29:605–621.

Fish, F. E., and J. M. Battle. 1995. Hydrodynamic design of the humpback whale flipper. Journal of Morphology 225:51–60.

Fish, F. E., and G. V. Lauder. 2006. Passive and active flow control by swimming fishes and mammals. Annual Review of Fluid Mechanics 38:193–224.

Fish, F. E., and J. Rohr 1999. Review of dolphin hydrodynamics and swimming performance. SPAWARS System Center Technical Report 1801, San Diego, CA. 196 pp.

Fish, F. E., J. E. Peacock and J. J. Rohr. 2003. Stabilization mechanism in swimming odontocete cetaceans by phased movements. Marine Mammal Science 19:515–528.

Fish, F. E., J. T. Beneski and D. R. Ketten. 2007. Examination of the three-dimensional geometry of cetacean flukes using computed tomography scans: Hydrodynamic implications. Anatomical Record 290:614–623.

Fish, F. E., L. E. Howle and M. M. Murray. 2008. Hydrodynamic flow control in marine mammals. Integrative and Comparative Biology 211:1859–1867.

Flórez-González, L., J. J. Capella and H. C. Rosenbaum. 1994. Attack of killer whales (*Orcinus orca*) on humpback whales (*Megaptera novaeangliae*) on a South American Pacific breeding ground. Marine Mammal Science 10:218–222.

Ford, J. K. B. 2009. Killer whale *Orcinus orca*. Pages 650–657 *in* W. F. Perrin, B. Würsig and J. G. M. Thewissen, eds. Encyclopedia of marine mammals. Academic Press, Amsterdam, The Netherlands.

Fox, R. W., and A. T. McDonald. 1999. Introduction to fluid mechanics, 5th ed. John Wiley & Sons, Inc., New York, NY.

Gambell, R. 1985. Fin whale *Balaenoptera physalus* (Linnaeus, 1758). Pages 171–192 *in* S. H. Ridgeway, and R. Harrison, eds. Handbook of marine mammals. Volume 3. The sirenians and baleen whales. Academic Press, London, U.K.

Geraci, J. R., and V. J. Lounsbury. 2005. Marine mammals ashore: A field guide for stranding, 2nd ed. National Aquarium in Baltimore, Baltimore, MD.

Goldbogen, J. A., J. Calambokidis, R. E. Shadwick, E. M. Oleson, M. A. McDonald and J. A. Hildebrand. 2006. Kinematics of foraging dives and lunge-feeding in fin whales. Journal of Experimental Biology 209:1231–1244.

Goldbogen, J. A., N. D. Pyenson and R. E. Shadwick. 2007. Big gulps require high drag for fin whale lunge feeding. Marine Ecology Progress Series 349:289–301.

Goldbogen, J. A., J. Calambokidis, A. S. Friedlaender, *et al.* 2012. Underwater acrobatics by the world's largest predator: 360° rolling manoeuvres by lunge-feeding blue whales. Biology Letters. doi:10.1098/rsbl.2012.0986.

Guinet, C., and J. Bouvier. 1995. Development of intentional stranding hunting techniques in killer whale (*Orcinus orca*) calves at Crozet Archipelago. Canadian Journal of Zoology 73:27–33.

Hoerner, S. F., and H. V. Borst. 1985. Fluid-dynamic lift. 2nd edition. Published by Author, Bakersfield, CA.

Howell, A. B. 1930. Aquatic mammals. Charles C, Thomas, Springfield, IL.

Jefferson, T. A., P. J. Stacey and R. W. Baird. 1991. A review of killer whale interactions with other marine mammals: Predation to co-existence. Mammal Review 21:151–180.

Johannessen, C. L., and J. A. Harder. 1960. Sustained swimming speeds of dolphins. Science 132:1550–1551.

Lockyer, C. 1977. Observations on the diving behavior of the sperm whale, *Physeter catodon*. Pages 591–609 *in* M. Angel, ed. A voyage of discovery. Pergamon Press, Oxford, U.K.

Maresh, J. L., F. E. Fish, D. P. Nowacek, S. M. Nowacek and R. S. Wells. 2004. High performance turning capabilities during foraging by bottlenose dolphins. Marine Mammal Science 20:498–509.

Marino, L., M. D. Uhen, N. D. Pyenson and B. Frohlich. 2003. Reconstructing cetacean brain evolution using computed tomography. Anatomical Record 272B:107–117.

Miklosovic, D. S., M. M. Murray, L. E. Howle and F. E. Fish. 2004. Leading-edge tubercles delay stall on humpback whale (*Megaptera novaeangliae*) flippers. Physics of Fluids 16: L39–L42.

Miller, P. J. O., M. P. Johnson, P. L. Tyack and E. A. Terray. 2004. Swimming gaits, passive drag and buoyancy of diving sperm whales *Physeter macrocephalus*. Journal of Experimental Biology 207:1953–1967.

Murray, M. M., D. A. Miklosovic, F. E. Fish and L. E. Howle 2005. Effects of leading edge tubercles on a representative whale flipper model at various sweep angles. Conference Proceedings of the 14th International Symposium on Unmanned Untethered Submersible Technology, Durham, NH.

Norris, K. S., and G. W. Harvey. 1972. A theory for the function of the spermaceti organ of the sperm whale (*Physeter catodon* L.). Pages 397–417 *in* S. R. Galler, K. Schmidt-Koenig, G. J. Jacobs, and R. E. Belleville, eds. Animal orientation and navigation. National Aeronautic and Space Administration, Washington, DC.

Norris, K. S., and B. Møhl. 1983. Can odontocetes debilitate prey with sound? American Naturalist 122:85–104.

Papastavrou, V., S. C. Smith and H. Whitehead. 1989. Diving behaviour of the sperm whale, *Physeter macrocephalus*, off the Galapagos Islands. Canadian Journal of Zoology 67:839–8846.

Pitman, R. L., L. T. Ballance, S. Mesnick and S. Chivers. 2001. Killer whale predation on sperm whales: Observations and implications. Marine Mammal Science 17:494–507.

Pitman, R. L., S. O. O'Sullivan and B. Mase. 2003. Killer whales (*Orcinus orca*) attack a school of Pantropical spotted dolphins (*Stenella attenuata*) in the Gulf of Mexico. Aquatic Mammals 29:321–324.

Pitman, R. L., and J. W. Durban. 2012. Cooperative hunting behavior, prey selectivity and prey handling by pack ice killer whales (*Orcinus orca*), type B, in Antarctic Peninsula waters. Marine Mammal Science 28:16–36.

Pivorunas, A. 1979. The feeding mechanisms of baleen whales. American Scientist 67:432–440.

Reeves, P. A., B. S. Stewart, P. J. Clapham and J. A. Powell. 2002. Guide to marine mammals of the world. Alfred A, Knopf, New York, NY.

Rice, D. W. 1989. Sperm whale *Physeter macrocephalus* Linnaeus, 1758. Pages 177–233 *in* S. H. Ridgeway, and R. Harrison, eds. Handbook of marine mammals. Volume 4. River dolphins and the larger toothed whales. Academic Press, London, U.K.

Rohr, J., M. I. Latz, E. Hendricks and J. C. Nauen. 1995. A novel flow visualization technique using bioluminescent marine plankton. Part II: Field studies. IEEE Journal of Oceanographic Engineering 20:147–149.

Rohr, J., M. I. Latz, S. Fallon, J. C. Nauen and E. Hendricks. 1998. Experimental approaches towards interpreting dolphin-stimulated bioluminescence. Journal of Experimental Biology 201:1447–1460.

Sanchez, J. A., and A. Berta. 2010. Comparative anatomy and evolution of the odontocete forelimb. Marine Mammal Science 26:140–160.

Schultz, M. P., and K. A. Flack. 2005. Outer layer similarity in fully rough turbulent boundary layers. Experiment in Fluids 38:328–340.

Shaughnessy, E. J., I. M. Katz and J. P. Schaffer. 2005. Introduction to fluid mechanics. Oxford University Press, New York, NY.

Silber, G. K., M. W. Newcomer and H. Perez-Cortes. 1990. Killer whales (*Orcinus orca*) attack and kill a Bryde's whale (*Balaenoptera edeni*). Canadian Journal of Zoology 68:1603–1606.

Similä, A. 1997. Sonar observations of killer whales (*Orcinus orca*) feeding on herring schools. Aquatic Mammals 23:119–126.

Similä, A., and F. Ugarte. 1993. Surface and underwater observations of cooperatively feeding killer whales in northern Norway. Canadian Journal of Zoology 71:1494–1499.

Springer, A. M., J. A. Estes, G. B. van Vliet, *et al.* 2003. Sequential megafaunal collapse in the North Pacific Ocean: An ongoing legacy of industrial whaling? Proceedings of the National Academy of Sciences of the United States of America 100:12223–12228.

Stimpert, A. K., D. N. Wiley, W. W. L. Au, M. P. Johnson and R. Arsenault. 2007. 'Megaclicks': Acoustic click trains and buzzes produced during night-time foraging of humpback whales (*Megaptera novaeangliae*). Biology Letters 3:467–470.

Thewissen, J. G. M. 1998. The emergence of whales. Plenum Press, New York, NY.

Tomilin, A. G. 1957. Mammals of the U.S.S.R. and adjacent countries. Volume IX. Cetacea. Nauk S.S.S.R., Moscow, Russia (English translation, 1967, Israel Program for Scientific Translations, Jerusalem, Israel).

von Mises, R. 1945. Theory of flight. Dover, New York, NY.

Watkins, W. A., M. A. Daher, K. M. Fristrup, T. J. Howald and G. Notarbartolo Di Sciara. 1993. Sperm whales tagged with transponders and tracked underwater by sonar. Marine Mammal Science 9:55–67.

Webb, P. W. 1975. Hydrodynamics and energetics of fish propulsion. Bulletin of the Fisheries Research Board of Canada 190:1–158.

Weber, P. W., M. M. Murray, L. E. Howle and F. E. Fish. 2009*a.* Comparison of real and idealized cetacean flippers. Bioinspiration and Biomimetics 4:046001.

Weber, P. W., L. E. Howle, M. M. Murray and F. E. Fish. 2009*b.* Lift and drag performance of odontocete cetacean flippers. Journal of Experimental Biology 212:2149–2158.

Werth, A. J. 2004. Functional morphology of the sperm whale (*Physeter macrocephalus*) tongue, with reference to suction feeding. Aquatic Mammals 30:405–418.

Whitehead, H. 2003. Sperm whales: Social evolution in the ocean. Chicago University Press, Chicago, IL.

Whitehead, H. 2009. Sperm whale *Physeter macrocephalus*. Pages 1091–1097 *in* W. F. Perrin, B. Würsig and J. G. M. Thewissen, eds. Encyclopedia of marine mammals. Academic Press, Amsterdam, The Netherlands.

Wiley, D. N., C. Ware, A. Bocconcelli, D. Cholewiak, A. Friedlaender, M. Thompson and M. Weinrich. 2011. Underwater components of humpback whale bubble-net feeding behavior. Behaviour 148:575–602.

Williamson, G. R. 1972. The true body shape of rorqual whales. Journal of Zoology, London 167:277–286.

Woodward, B. L., J. P. Winn and F. E. Fish. 2006. Morphological specializations of baleen whales associated with hydrodynamic performance and ecological niche. Journal of Morphology 267:1284–1294.

Yochem, P. K., and S. Leatherwood. 1985. Blue whale *Balaenoptera musculus* Linnaeus, 1758. Pages 193–240 *in* S. H. Ridgeway, and R. Harrison, eds. Handbook of marine mammals Volume 3. The sirenians and baleen whales. Academic Press, London, U.K.

Zimmer, W. M. X., M. P. Johnson, A. D'Amico and P. L. Tyack. 2003. Combining data from a multisensory tag and passive sonar to determine the diving behavior of a sperm whale (*Physeter macrocephalus*). IEEE Journal of Oceanic Engineering 28:13–28.

Received: 27 December 2012
Accepted: 25 March 2013